Small-Angle X-ray Scattering Study of Calmodulin Bound to Two Peptides Corresponding to Parts of the Calmodulin-Binding Domain of the Plasma Membrane Ca^{2+} Pump†

Mikio Kataoka,‡ James F. Head,*,§ Thomas Vorherr,∥ Joachim Krebs,∥ and Ernesto Carafoli∥

Department of Physics, Tohoku University, Aramaki, Aoba-ku, Sendai 980, Japan, Department of Physiology, Boston University School of Medicine, Boston, Massachusetts 02118, and Department of Biochemistry, Swiss Federal Institute of Technology (ETH), Zurich, Switzerland

Received December 31, 1990; Revised Manuscript Received March 28, 1991

ABSTRACT: The interaction between calmodulin (CaM) and two synthetic peptides, C20W and C24W, corresponding to parts of the calmodulin-binding domain of the Ca^{2+} pump of human erythrocytes, has been studied by using small-angle X-ray scattering (SAXS). The total length of the CaM-binding domain of the enzyme is estimated to be 28 amino acids. C20W contains the 20 N-terminal amino acids of this domain, C24W the 24 C-terminal amino acids. The experiments have shown that the binding of either peptide results in a complex with a radius of gyration (R_g) smaller than that of CaM. The complex between CaM and C20W revealed an interatomic length distribution function, $P(r)$, similar to that of calmodulin alone, indicating that the complex retains an extended, dumbbell-shaped structure. By contrast, the binding of C24W resulted in the formation of a globular structure similar to those observed with many other CaM-binding peptides.

The crystal structure of calmodulin (Babu et al., 1985, 1988; Kretsinger et al., 1986) has revealed a number of features thought to be necessary to the function of the protein. Four homologous "helix–loop–helix" calcium-binding domains (Kretsinger, 1980) are arranged in pairs to form two globular regions that are connected by a seven-turn α-helix, much of which is solvent exposed. Flexibility in this central helix has been proposed as a means by which the two lobes of calmodulin may be brought into apposition on target peptides (Heidorn & Trewhella, 1988; Persechini & Kretsinger, 1988a,b; Kataoka et al., 1989; Yoshino et al., 1989; Matsushima et al., 1989; Heidorn et al., 1989). Binding is believed to occur, at least in part, through calcium-dependent hydrophobic surface domains on each lobe (LaPorte et al., 1980; Tanaka & Hidaka, 1980; Krebs et al., 1984). In this model, the calmodulin molecule undergoes a dumbbell to globular shape transition on binding to the target.

Small-angle X-ray scattering (SAXS)[1] can provide information on the overall shape of proteins in solution (Pilz, 1982). In spite of its low resolution, it can enable models to be proposed for the overall three-dimensional shape of protein molecules, and it can enable testing of models based on other techniques. SAXS studies have confirmed that calmodulin exists as a dumbbell structure not only in crystals but also in free solution (Seaton et al., 1985; Heidorn & Trewhella, 1988). It has also demonstrated changes in the radius of gyration and the maximum dimension of the molecule on binding calcium (Seaton et al., 1985; Heidorn & Trewhella, 1988). Even more strikingly, the transition from the dumbbell shape to a more compact globular conformation, described above, has been demonstrated when calmodulin binds to several known calmodulin-binding peptides (Kataoka et al., 1989; Yoshino et al., 1989; Matsushima et al., 1989; Heidorn et al., 1989). The effects of mutations of calmodulin on the conformation of the protein and its peptide complexes have also been studied with this technique (Kataoka et al., 1991).

Many calmodulin-binding peptides and calmodulin-binding domains of regulated enzymes share a structure consisting of a basic amphipathic helix (Blumenthal et al., 1985). In the present study, the solution structure of calmodulin bound to peptides corresponding to parts of the calmodulin-binding domain of the Ca^{2+} pump of human erythrocytes has been studied (Verma et al., 1988). This domain consists of 28 residues, has a propensity to form an amphipathic helix (James et al., 1988), and displays a helix plus β-sheet arrangement, as determined by CD methods (Vorherr et al., 1990). Several peptides based on this sequence have been synthesized, and their interaction with calmodulin has been characterized by CD and NMR techniques (Vorherr et al., 1990). These studies suggest that a shorter version of the domain, peptide C20W, interacts solely with the C-terminal region of the calmodulin dumbbell. In the present work, the overall conformation of calmodulin complexed with two of these synthetic peptides, C24W and C20W, has been studied. The results indicate that

† This work was supported in part by a grant from the Ministry of Education, Science and Culture of Japan to M.K. (02680217), a grant from the United States National Institutes of Health to J.F.H. (NS 20357), and a grant from the Swiss National Science Foundation to E.C. (31.25285.88). Small-angle X-ray scattering experiments using synchrotron radiation were performed at the Photon Factory, Tsukuba, Japan, under the approval of the Program Advisory Committee (proposal 90-060).

* Address correspondence to this author at the Department of Physiology, Boston University School of Medicine, 80 E. Concord St., Boston, MA 02118.

‡ Department of Physics, Tohoku University, Aramaki, Aoba-ku, Sendai 980, Japan.

§ Department of Physiology, Boston University School of Medicine, Boston, MA.

∥ Department of Biochemistry, Swiss Federal Institute of Technology (ETH), Zurich, Switzerland.

[1] Abbreviations: CaM, calmodulin; DCC, dicyclohexylcarbodiimide; DVB, divinylbenzol; Fmoc, 9-fluorenylmethyloxycarbonyl; HOBt, 1-hydroxybenzotriazole; HPLC, high-performance liquid chromatography; NMP, *N*-methylpyrrolidone; NMR, nuclear magnetic resonance; Pmc, 2,2,5,7,8-pentamethylchroman-6-sulfonyl; PTC, phenyltriocarbamyl; PTH, phenylthiohydantoin; R_g, radius of gyration; SAXS, small-angle X-ray scattering; tBu, tertiary butyl; TFA, trifluoroacetic acid.

0006-2960/91/0430-6247$02.50/0

the binding of peptide C20W to calmodulin does not significantly alter the extended structure of calmodulin, whereas the complex with peptide C24W forms a globular structure.

Materials and Methods

Protein and Peptide Isolation. Calmodulin was purified from bovine brain by the method of Masure et al. (1984). The calmodulin-binding peptide C20W was synthesized as described elsewhere (Vorherr et al., 1990).

Synthesis and Purification of C24W. The peptideamide Q-I-L-W-F-R-G-L-N-R-I-Q-T-Q-I-R-V-V-N-A-F-R-S-S-NH_2 was synthesized on an Applied Biosystems (Foster City, CA) peptide synthesizer model 431 employing the Fmoc/tBU strategy with 1-methyl-2-pyrrolidone for coupling and washing according to the standard protocol for this machine. The peptide sequence is that contained in the hPMCA1b isoform of the Ca^{2+} ATPase (Verma et al., 1988). The first amino acid was attached according to the standard cycle after removal of the Fmoc protecting group of the acid-labile amide-anchoring group (Rinke, 1987) [4-[2′,4′-dimethoxyphenyl(9-fluorenylmethyloxycarbonyl)aminomethyl]phenoxy resin] attached to the Tentagel resin (Rapp Polymere, Tuebingen, Germany). The peptide was synthesized by using Pmc protection for the Arg residues and trityl protection for the Asn and Gln residues starting with 0.16 mmol of resin (1% DVB, polyoxyethylene spacer, 0.22 mmol/g) and a 6.2-fold excess of the amino acid derivative. A capping cycle, employing acetanhydride after each coupling, was performed according to the instructions of the manufacturer. Cleavage of the peptide was performed in a mixture of 1.5 mL of TFA, 50 mL of ethanedithiol, 75 μL of water, 115 mg of phenol, and 75 μL of thioanisol for 1 h 40 min at room temperature. From 134 mg of Fmoc deprotected peptide resin, 38.5 mg of crude product was obtained after precipitation and washing with ethyl ether. From 38.5 mg of crude peptide, 6.9 mg of purified peptide was obtained after preparative HPLC using the buffers A (0.1% TFA in water) and B (0.05% TFA, 50% *n*-propanol in water). The amino acid analysis agreed with the expected ratios (Trp was not determined). The sequence analysis confirmed the sequence and showed the intact Trp residue.

HPLC Analysis, Amino Acid Analysis, and Sequencing of the Peptides. Preparative and analytical HPLC were carried out with Nucleosil reversed-phase materials packed in Macherey & Nagel columns (Oensingen, Switzerland). Buffers A and B were used for reverse-phase HPLC. The peptides were purified on a 250 × 55 mm C8 column (10 μm, 300 Å) by applying a linear gradient from A to B. The flow rate was 21 mL/min. An analytical control was performed on a 60 × 4 mm C8 column (5 μm, 300 Å) in the same solvent system. Chromatography was carried out with Applied Biosystems and LKB equipment (LKB, Uppsala, Sweden). UV detection for analytical control was performed at 206 nm. Sequencing was carried out with an Applied Biosystems 470A sequencer with 120A on-line PTH detection. An Applied Biosystems 420A derivatizer and on-line PTC detection with the model 130A Applied Biosystems analyzer was used for derivatization, separation, and identification of the amino acids.

Sample Preparation. C20W and C24W peptides were dissolved in 0.1% TFA, and calmodulin was dissolved in water. The concentration of the solutions was determined by quantitative amino acid analysis. Samples of calmodulin alone and mixed with equimolar amounts of peptide were dialyzed in a Spectrapor 4 dialysis membrane against two changes each of 100 volumes of 100 mM KCl, 50 mM MOPS, and 0.02% sodium azide (pH 7.4). The first dialysis included either 1 mM $CaCl_2$, for samples to be analyzed in the presence of calcium, or 5 mM EGTA, for those samples to be analyzed in the absence of calcium. In the second dialysis these concentrations were dropped to 0.1 mM $CaCl_2$ and 1 mM EGTA. Dialysis fluids for samples containing peptides also included 1 μM peptide. After dialysis, the final concentration of protein was redetermined by quantitative amino acid analysis. Concentration series were prepared by diluting the dialyzed sample with the final dialysis fluid.

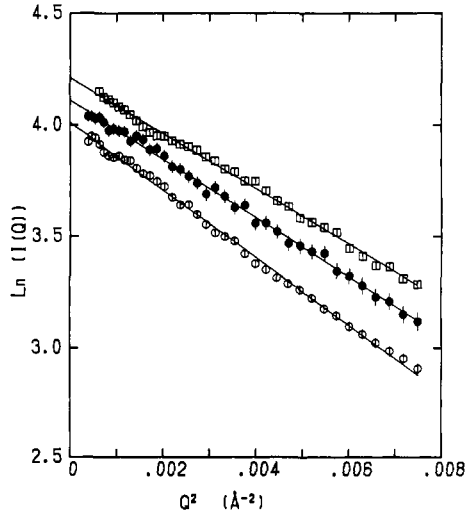

FIGURE 1: Guinier plots of small-angle scattering data extrapolated to zero concentration. Symbols: (○) calmodulin alone, (●) calmodulin–C20W complex, and (□) calmodulin–C24W complex. All samples contained 0.1 mM Ca^{2+}.

Small-Angle X-ray Scattering. Small-angle X-ray scattering measurements were performed by using the solution-scattering station installed at BL10C at the Photon Factory, Tsukuba, Japan with synchrotron radiation. The wavelength of the X-rays was adjusted to 1.488 Å, calibrated by the nickel absorption edge. The incident beam was focused by a bent cylindrical mirror to give a quasi-point focus. The detailed design and performance of the station are described elsewhere (Ueki et al., 1985).

The samples were measured with a specially designed cell with quartz windows that were 10 μm thick, 10 mm wide, and 5 mm high. The path length was 1 mm. Samples were maintained at 20 °C by circulating thermostated water through the cell holder. The specimen to detector distance was near 90 cm and was calibrated by the meridional diffraction from dried chicken collagen. Exposure times ranged from 10 to 15 min depending on the protein concentration. The incident intensity was measured by an ionizing chamber placed in front of the specimen cell holder during each exposure to normalize each set of scattering data. Scattering profiles were recorded by a 20-cm long linear position-sensitive detector (Rigaku, Tokyo). The final dialysis fluid of each protein sample was used to determine background scatter.

Data analysis. The small-angle X-ray scattering intensity distribution from a protein in solution is expressed by

$$I(Q) \propto \exp(-R_g^2 Q^2/3)$$

where $Q = (4\pi \sin \Theta)/\lambda$ and 2Θ and λ are the scattering angle and wavelength of the X-rays (Guinier & Fournet, 1955). Thus, the Guinier plot, ln $I(Q)$ vs Q^2, should approximate a straight line in the small-angle region with a slope of R_g (e.g., see Figure 1).

Scattering curves at infinite dilution were obtained by linear extrapolation of a series of scattering curves obtained at five

Table I: Amino Acid Sequence of the Synthetic Peptides Based on the Sequence of the Calmodulin-Binding Domain of the Ca^{2+}–Mg^{2+} ATPase of Red Blood Cell Plasma Membrane

CaM-binding domain[a]	LRRGQILWFRGLNRIQTQIRVVNAFRSS
C24W	QILWFRGLNRIQTQIRVVNAFRSS
C20W	LRRGQILWFRGLNRIQTQIK

[a] This sequence corresponds to the full calmodulin-binding region of the hPMCA1b isoform of the Ca^{2+} ATPase (Verma et al., 1988) and is shown for reference.

Table II: Structural Parameters Obtained by SAXS for Calmodulin and the Calmodulin–Peptide Complexes in the Presence of Calcium[a]

	R_g Guinier (Å)	R_g Moore (Å)	d_{max} (Å)	$I(0)^b$	predicted $I(0)$
CaM	21.36 (0.10)	22.01 (0.09)	62.5 (2.5)	1.00 (0.01)	1
CaM + C20W	19.62 (0.18)	19.77 (0.15)	57.5 (2.5)	1.16 (0.01)	1.15
CaM + C24W	18.87 (0.03)	18.95 (0.04)	52.5 (2.5)	1.21 (0.01)	1.16

[a] Errors are in parentheses. [b] $I(0)$ value relative to calmodulin alone.

or more protein concentrations. Extrapolations were made by direct extrapolation and by using Zimm plots. Both methods gave essentially the same final scattering curves. Final extrapolated data were analyzed by Guinier analysis (Guinier & Fournet, 1955) or the indirect Fourier transform method of Moore (1980). The details of the analysis techniques have been described previously (Kataoka et al., 1989, 1991).

Results

The binding of either C20W or C24W (see Table I) to calmodulin was found to result in the formation of a complex that has a smaller R_g than calmodulin alone. However, the extent of the change was different for each peptide. Figure 1 shows Guinier plots for calmodulin alone, calmodulin + C20W, and calmodulin + C24W, each in the presence of calcium. The slope of the Guinier plot at small angles is a function of R_g. As can be seen, each plot has a distinct slope, indicative of a different R_g value. The R_g values obtained from these plots are summarized in Table II.

Apparent R_g values are dependent on protein concentration, due to interparticle interference. In order to obtain the value for R_g at zero concentration, the intensity function extrapolated to zero concentration was obtained from a series of scattering measurements made at five different protein concentrations ranging from approximately 3 to 20 mg/mL. The Guinier plots in Figure 1 were created from the extrapolated scattering function. The R_g value at zero concentration can also be calculated by extrapolating a plot of the square of the apparent R_g value at each concentration vs concentration (Zaccai & Jacrot, 1983). Values obtained by either method were essentially the same.

Data analysis by the method of Moore (1980), which includes a slit-desmearing correction, often gives R_g values that differ a little from those obtained by the Guinier analysis; however, since the optics used in these studies was a pseudo-point focusing system, the values obtained by the two procedures are very similar in this case (Table II). The intensity of scattering at 0°, or forward scattering, $I(0)$, is a function of the molecular weight of the scattering entity and as such is a sensitive measure of aggregation. No evidence of aggregation was observed in any of the samples of calmodulin–peptide in the presence of calcium. As shown in Table II, the $I(0)$ of the peptide complexes relative to calmodulin alone are

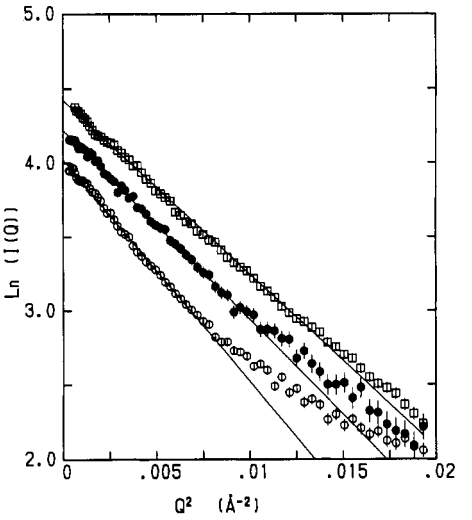

FIGURE 2: Extended Guinier plots of scattering data extrapolated to zero concentration. Symbols: (○) calmodulin alone, (●) calmodulin–C20W complex, and (□) calmodulin–C24W complex. All data were taken in the presence of Ca^{2+}. Inflections in plots for calmodulin alone and calmodulin–C20W occur at around $Q^2 \approx 0.01$. $I(0)$ values for each plot have been displaced from one another for the sake of clarity.

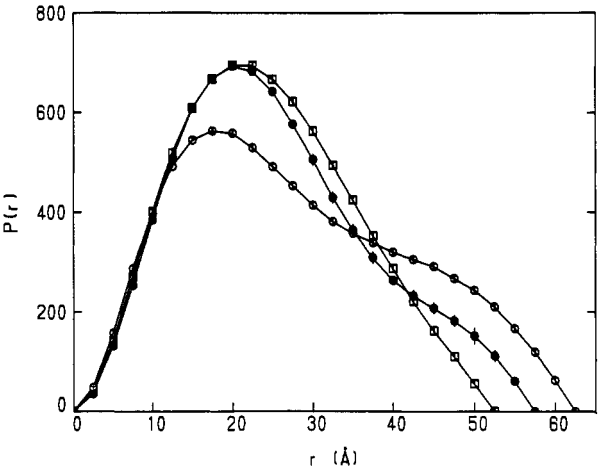

FIGURE 3: Interatomic length distribution function, $P(r)$. Symbols: (○) calmodulin alone, (●) calmodulin–C20W complex, and (□) calmodulin–C24W complex. The $P(r)$ functions were derived by the indirect Fourier transform method of Moore (1980), with the data shown in Figure 2.

slightly higher, consistent with the molecular weight increase resulting from the binding of one mole of peptide per mole of calmodulin.

Since the calmodulin–C20W complex has a larger R_g than the calmodulin–C24W complex, it is evident they are distinct structures. The structural differences are further manifested in differences in the intensity functions in higher angle regions (Figure 2). Figure 2 shows extended Guinier plots. The inflections in the curves at $Q^2 \approx 0.01$ for calmodulin alone and for the calmodulin–C20W complex are apparent and are indicative of dumbbell-shape structures (Fujisawa et al., 1987). However, the plot for the calmodulin–C24W structure is almost linear, suggesting a globular structure. Similar conclusions can be drawn from the related interatomic length distribution functions, $P(r)$, shown in Figure 3. Calmodulin alone has a peak of interatomic distances near 20 Å, principally representing interatomic distances within each lobe of the dumbbell, and a shoulder at about 45 Å, representing interlobe distances. The maximum length is about 63 Å. The calmodulin–C20W complex has a distribution function with a similar

form, indicative of a dumbbell, but with a maximum length of only about 58 Å. The complex of calmodulin with C24W has a very much different $P(r)$ function. The single peak with no shoulder is consistent with the profiles previously observed for the calmodulin–melittin complex (Kataoka et al., 1989) and is interpreted as representing a globular complex.

In addition to the measurements made on samples containing calcium, we also measured SAXS using samples containing EGTA, that is, in the absence of significant free Ca^{2+}. Under these conditions, we experienced problems of aggregation and precipitation, each sample including a white precipitate. SAXS data from such samples showed a steep upward slope in the Guinier plots of the small-angle region, indicative of aggregation. Under these conditions, the extended Guinier plots all showed inflections near $Q^2 = 0.01$ suggesting remaining solute in the dumbbell form. After removal of the precipitate by centrifugation, the samples gave scattering data consistent with calmodulin alone in the absence of calcium. Amino acid analyses of the supernatant samples are also consistent with calmodulin containing little or no peptide. We conclude that the peptides, which on their own have poor solubilities under these conditions, dissociate from calmodulin in the absence of calcium and precipitate.

Discussion

Both C20W and C24W induce a Ca^{2+}-dependent conformational change in calmodulin. However, the solution structures of the complexes are different. The calmodulin–C20W complex appears to be a dumbbell shape, while the calmodulin–C24W complex is globular. In forming a globular complex, C24W appears to fall in to the same group as the calmodulin-binding peptides melittin (Kataoka et al., 1989), mastoparan (Matsushima et al., 1989; Yoshino et al., 1989), and the M13 peptide derived from the calmodulin-binding domain of myosin light chain kinase (Heidorn et al., 1989).

Since the calmodulin–C20W structure appears to be unusual, the basis for our interpretation of the structure has to be examined carefully. SAXS measurements give information on an average of structures in solution over time. One possible interpretation of the results for the C20W complex is therefore that the solute is polydisperse, some globular complex mixed with unliganded calmodulin, thus giving the average structure of a more compact dumbbell. We believe this is unlikely to be the case for several reasons. Samples were prepared by mixing equimolar amounts of the peptide and calmodulin and dialyzed against solutions containing 1 μM peptide. With a K_d for the complex of 11 nM (Vorherr et al., 1990), this treatment should ensure that the calmodulin is nearly saturated with peptide. This conclusion is supported by the amino acid analyses of the dialyzed samples, which indicate the presence of 1 mol each of peptide and calmodulin. The scattering measurements themselves also suggest a monodisperse species, and the relative $I(0)$ of the complex is consistent with the expected molecular weight of equimolar calmodulin and C20W. The compacted dumbbell shape therefore appears to represent the intact complex. It is possible that the complex itself undergoes dynamic changes between an extended and a globular structure, giving a time-averaged compacted dumbbell shape. This itself would be clearly distinct from the complexes formed with melittin, mastoparan, M13, and C24W. The remaining alternative is that the complex maintains the compacted dumbbell structure in solution.

NMR studies by Vorherr et al. (1990) indicate that C20W interacts only with one lobe of calmodulin, as opposed to the M13 peptide of myosin light chain kinase and mastoparan, which have been shown by NMR to interact with both lobes of calmodulin (Klevit et al., 1985; Yazawa et al., 1987). The dumbbell to globular transition previously observed with calmodulin on binding peptides has been interpreted as being consistent with the model of Persechini and Kretsinger (1988a) in which the central helix of calmodulin bends, permitting the two lobes of calmodulin to rotate into place to enfold the target peptide. It appears from the results of Vorherr et al. (1990) and those of this study that C20W is not enfolded in this manner. The details of the molecular complex formed between C20W and calmodulin cannot be assessed by SAXS; however, we note with interest that the R_g and d_{max} of the calmodulin–C20W complex are very similar to those of a deletion mutant of calmodulin, des2, in which Glu83 and Glu84 have been deleted (Kataoka et al., 1991). In the case of des2, the reduced R_g and d_{max} were interpreted as reflecting both a reduction of the length of the central helix and also a relative rotation of the two lobes of calmodulin with respect to the central helix, from a trans to a cis orientation. While speculative, it is possible that the binding of C20W could cause a relative rotation of the C-terminal lobe to be cis with respect to the N-terminal lobe, thus reducing d_{max}.

C24W is similar in its properties to the entire 28-residue calmodulin-binding domain. The regulated enzyme complex may therefore include calmodulin bound in the globular conformation. It is possible that the apparently anomalous binding of C20W to only one calmodulin lobe may in fact represent the first step in the binding of the native peptide to form the physiological complex and thus provide an opportunity to study a conformation not normally readily accessible. Since the compacted dumbbell shape of the C20W complex represents a possible alternative conformation for calmodulin–peptide complexes, it could also provide an example of a conformation that may be physiologically exploited in the regulation of other enzyme systems.

During preparation of this manuscript, Trewhella et al. (1990) published a SAXS and neutron-scattering study of the solution structure of calmodulin complexed with synthetic peptides based on the calmodulin-binding domain of the regulatory subunit of phosphorylase kinase. There is an interesting parallel between the results obtained with the phosphorylase kinase peptides and those of the plasma membrane Ca^{2+} ATPase; one peptide from each enzyme is found to form a dumbbell-shaped complex with calmodulin. This is of considerable importance, since it indicates that a globular complex is only one of the possible conformations available to calmodulin on binding to targets rather than the sole structure, as seemed likely from earlier studies. However, beyond this parallel there appears to be little other similarity between the sets of peptides. In the case of phosphorylase kinase, the PhK13 peptide, which forms an extended dumbbell-shaped complex with calmodulin, is present in the intact protein in addition to, but at a distance from, the PhK5 peptide, which forms a globular-type complex. In the case of the membrane Ca^{2+} ATPase, the peptide able to form an extended complex, C20W, overlaps with the peptide able to form a globular complex, C24W. The overall shape of the dumbbell complex formed with PhK13 and C20W also seems to be different, the former being longer than calmodulin alone, the latter shorter. The PhK13 peptide appears to be predominantly a β-turn/β-sheet structure based on secondary structure predictions, whereas C20W appears to be mostly helical, as determined by CD measurements (Vorherr et al., 1990). Despite these differences, both the PhK13 and the C20W peptides provide a valuable opportunity to study the structural requirements for the formation of the calmodulin–

target complex and to explore some of the possible alternatives.

Registry No. C24W, 133850-19-8; ATPase, 9000-83-3.

REFERENCES

Babu, Y. S., Sack, J. S., Greenhough, T. C., Bugg, C. E., Means, A. R., & Cook, W. J. (1985) *Nature 315*, 37.

Babu, Y. S., Bugg, C. E., & Cook, W. J. (1988) *J. Mol. Biol. 204*, 191.

Blumenthal, D. K., Takio, K., Edelman, A. M., Charbonneau, H., Titani, K., Walsh, K. A., & Krebs, E. G. (1985) *Proc. Natl. Acad. Sci. U.S.A. 82*, 3187.

Fujisawa, T., Ueki, T., Inoko, T., & Kataoka, M. (1987) *J. Appl. Crystallogr. 20*, 349.

Guinier, A., & Fournet, G. (1955) in *Small-Angle Scattering of X-rays*, J. Wiley, New York.

Heidorn, D. B., & Trewhella, J. (1988) *Biochemistry 27*, 909.

Heidorn, D. B., Seeger, P. A., Rokop, S. E., Blumenthal, D. K., Means, A. R., Crespi, H., & Trewhella, J. (1989) *Biochemistry 28*, 6757.

James, P., Maeda, M., Fischer, R., Verma, A. K., Krebs, J., Penniston, J. T., & Carafoli, E. (1988) *J. Biol. Chem. 263*, 2905.

Kataoka, M., Head, J. F., Seaton, B. A., & Engelman, D. M. (1989) *Proc. Natl. Acad. Sci. U.S.A. 86*, 6944.

Kataoka, M., Head, J. F., Persechini, A., Kretsinger, R. H., & Engelman, D. M. (1991) *Biochemistry 30*, 1188.

Klevit, R. E., Blumenthal, D. K., Wemmer, D. E., & Krebs, E. G. (1985) *Biochemistry 24*, 8152.

Krebs, J., Buerkler, J., Guerini, D., Brunner, J., & Carafoli, E. (1984) *Biochemistry 23*, 400.

Kretsinger, R. H. (1980) *CRC Crit. Rev. Biochem. 8*, 119.

Kretsinger, R. H., Rudnick, S. E., & Weissman, L. J. (1986) *J. Inorgan. Biochem. 28*, 289.

LaPorte, D. C., Wierman, B. M., & Storm, D. R. (1980) *Biochemistry 19*, 3814.

Masure, H. R., Head, J. F., & Tice, H. (1984) *Biochem. J. 218*, 891.

Matsushima, N., Izumi, Y., Matsuo, T., Yoshino, Y., Ueki, T., & Miyake, Y. (1989) *J. Biochem. (Tokyo) 105*, 883.

Moore, P. B. (1980) *J. Appl. Crystallogr. 13*, 168.

Persechini, A., & Kretsinger, R. H. (1988a) *J. Cardiovasc. Pharmacol. 12 (Suppl. 5)*, S1.

Persechini, A., & Kretsinger, R. H. (1988b) *J. Biol. Chem. 263*, 12175.

Pilz, I. (1982) in *Small-Angle X-ray Scattering* (Glatter, O., & Kratky, O., Eds.) pp 239–293, Academic Press, New York.

Rinke, H. (1987) *Tetrahedron Lett. 28*, 3787.

Seaton, B. A., Head, J. F., Engelman, D. M., & Richards, F. M. (1985) *Biochemistry 24*, 6740.

Tanaka, T., & Hidaka, H. (1980) *J. Biol. Chem. 255*, 11078.

Trewhella, T., Blumenthal, D. K., Rokop, S. E., & Seeger, P. A. (1990) *Biochemistry 29*, 9316.

Ueki, T., Hiragi, Y., Kataoka, M., Inoko, Y., Amemiya, Y., Izumi, Y., Tagawa, H., & Muroga, Y. (1985) *Biophys. Chem. 23*, 115.

Verma, A. K., Filoteo, A. G., Standord, D. R., Wieben, E. D., Penniston, J. T., Streher, E. E., Fischer, R., Helm, R. Vogel, G., Mathews, S., Streher-Page, M.-A., James, P., Vorherr, T., Krebs, J., & Carafoli, E. (1988) *J. Biol. Chem. 263*, 14152.

Vorherr, T., James, P., Krebs, J., Enyedi, A., McCormick, D. J., Penniston, J. T., & Carafoli, E. (1990) *Biochemistry 29*, 355.

Yazawa, M., Ikura, M., Hikichi, K., Ying, L., & Yagi, K. (1987) *J. Biol. Chem. 262*, 10951.

Yoshino, H., Minari, O., Matsushima, N., Ueki, T., Miyake, Y., Matsuo, T., & Izumi, Y. (1989) *J. Biol. Chem. 264*, 19706.

Zaccai, G., & Jarcot, B. (1983) *Annu. Rev. Biophys. 12*, 139.